

Manuscript received October 5, 2024; Revised December 1, 2024; Accepted December 12, 2024; date of publication February 15, 2025  
Digital Object Identifier (DOI): <https://doi.org/10.35882/jeeemi.v7i2.629>

Copyright © 2025 by the authors. This work is an open-access article and licensed under a Creative Commons Attribution-ShareAlike 4.0 International License ([CC BY-SA 4.0](https://creativecommons.org/licenses/by-sa/4.0/)).

How to cite: Alan Samudra, Lutfatul Fitriana, Fathur Rachman Hidayat, Kurnanto Mukti Wibowo, Ariesma Githa Giovany and Wahyu Caesarendra, "Analysis of Differences in Image Quality and Anatomical Information of Head CT Scan Examination in Non-Hemorrhagic Stroke Cases Using Sinogram Affirmed Iterative Reconstruction (SAFIRE)", Journal of Electronics, Electromedical Engineering, and Medical Informatics, vol. 7, no. 2, pp. 270-282, April 2025.

# Analysis of Differences in Image Quality and Anatomical Information of Head CT Scan Examination in Non-Hemorrhagic Stroke Cases Using Sinogram Affirmed Iterative Reconstruction (SAFIRE)

Alan Samudra<sup>1</sup>, Lutfatul Fitriana<sup>1</sup>, Fathur Rachman Hidayat<sup>1</sup>, Kurnanto Mukti Wibowo<sup>2</sup>, Ariesma Githa Giovany<sup>3</sup>, and Wahyu Caesarendra<sup>4</sup>

<sup>1</sup> Department of Radiologic Imaging Technology, Universitas Muhammadiyah Purwokerto, Banyumas, Indonesia

<sup>2</sup> Department of Electromedical Engineering, Universitas Muhammadiyah Purwokerto, Banyumas, Indonesia

<sup>3</sup> Department of Radiology, Rumah Sakit Dr. Oen Kandang Sapi Solo, Surakarta, Indonesia

<sup>4</sup> Department of Mechanical and Mechatronics Engineering, Faculty of Engineering and Science, Curtin University Malaysia, Sarawak, Malaysia

Corresponding author: Lutfatul Fitriana (e-mail: [lutfatulfitriana@ump.ac.id](mailto:lutfatulfitriana@ump.ac.id))

**ABSTRACT** SAFIRE should be utilized to its full potential, as this innovative image reconstruction algorithm can significantly reduce image noise without loss of sharpness, preserving image quality and anatomical information. This is particularly important in the case of non-hemorrhagic stroke, where image noise can obscure small lesions, potentially leading to misdiagnosis and inappropriate treatment. SAFIRE has five variations of strength, making it essential to identify the most optimal SAFIRE Strength for head CT Scan examinations in non-hemorrhagic stroke cases. The aim of this study is to determine differences in image quality and anatomical information in head CT Scan of non-hemorrhagic stroke cases using SAFIRE variations to identify the most optimal SAFIRE Strength. This experimental quantitative study involved a sample of 30 patients, with each case reconstructed using five SAFIRE Strength variations. Image quality was assessed using the IndoQCT application, while anatomical information was evaluated through the visual grading analysis method by three radiologists. Image quality data were analyzed using the Friedman statistical test, which resulted in a p-value of 0.000 ( $p < 0.05$ ), indicating significant differences among the SAFIRE Strength variations. Similarly, anatomical information data were analyzed using the Kruskal-Wallis statistical test, yielding a p-value of 0.000 ( $p < 0.05$ ), confirming significant differences across the variations. The results of the study showed that there are significant differences in image quality and anatomical information among the five SAFIRE Strength variations. SAFIRE Strength 3 was identified as the most optimal for head CT Scan examinations in non-hemorrhagic stroke cases, as it produces images with minimal noise and higher detail, providing clearer anatomical information compared to the other SAFIRE Strength variations.

**INDEX TERMS** Head CT-Scan, Non-hemorrhagic Stroke, Image Quality, Anatomical Information.

## I. INTRODUCTION

In recent years, the use of Computed Tomography (CT) Scan has become increasingly prevalent in clinical practice, revolutionizing the way medical professionals diagnose and

treat a wide range of conditions. With its ability to provide fast, precise, and non-invasive imaging, CT Scan has proven invaluable in accurately assessing anatomical structures and detecting abnormalities. CT Scan for radiodiagnostic imaging

can measure differences or changes in the transmission of radiation across a targeted organ or body segment, allowing it to represent morphological aspects precisely. CT Scan produce fast and precise results, many medical professionals consider it an efficient and practical imaging technique to determine the type and severity of disease and help establish a diagnosis. Furthermore, it has been found that CT Scan contributes significantly to lowering the need for surgery by enabling alternative treatment recommendations, which lowers the surgery rate from 13% to 5%. [1][2]. Head CT Scan Examination is one of the most frequently performed procedures using CT Scan imaging.

Head CT Scan is a specialized imaging procedure of the head that utilizes tomographic techniques with X-ray beams passing through the patient's head from multiple angles. This process employs a computerized system to generate anatomical images in axial, sagittal, and coronal views [3]. Head CT Scan is recommended for a variety of conditions, including suspected neoplasms, brain metastases, strokes, aneurysms, intracranial bleeding, head atrophy, post-traumatic abnormalities, congenital anomalies, head injuries, and tumor masses or lesions.

Stroke is the second most common cause of mortality and a major contributor to disability worldwide [4][5][6]. Stroke also causes a large financial burden associated with pre-hospital, hospital, and post-hospital care costs [7], [8]. Based on its cause, stroke is classified into two types, namely non-hemorrhagic stroke or infarction and hemorrhagic stroke. The cause of infarction or non-hemorrhagic stroke is caused by embolism in the blood vessels of the brain, hemorrhagic stroke occurs due to a ruptured blood vessel in the brain [9]. Non-hemorrhagic stroke or infarction, also known as ischemic stroke accounts for 88% of all stroke cases. Ischemic stroke is associated with several major risk factors, including advanced age, hypertension, diabetes, hyperlipidemia, smoking, arrhythmia, and heart disease [10], [11], [12]. The clinical course of ischemic stroke is categorized into Reversible Ischemic Neurological Deficit (RIND), Transient Ischemic Attack (TIA), stroke in evolution, and completed stroke [13], [14], [15].

The increasing use of CT Scan has attracted significant attention, particularly on the exposure to radiation doses generated greater than other radiology modalities. According to the United States National Council on Radiation Protection and Measurements (NCRP), CT scans account for up to 24% of the radiation dose in medical imaging. Therefore, it is essential to minimize unnecessary variations in examination methods and reduce exposure to medical imaging [16]. On the other hand, what must be considered is that the lower the radiation dose will result in increased image noise, and the increasing noise, the image quality will decrease, and vice versa the higher the radiation dose, the lower the noise, the image quality will increase [17]. Noise is a random fluctuation of pixel values in an image [18]. Factors that influence the presence of noise are tube current (mA), tube voltage (kVp), tube rotation speed (s), slice thickness, type of image

reconstruction filter, etc. [19]. Therefore, it is crucial to identify a technique for lowering radiation exposure while preserving good image quality.

Image quality in CT Scan can be assessed by several parameters such as spatial resolution, contrast resolution, noise, and artifacts [17]. In addition, good image quality is characterized by high Signal to Noise Ratio (SNR) and high Contrast to Noise Ratio (CNR) [20], [21]. SNR is the ratio of signal intensity to background noise level, while CNR represents the capability to differentiate various tissue types based on their contrast differences. On the other hand, obtaining high-quality CT Scan images requires careful consideration of various factors and techniques, the quality of the equipment used, and the skill of the operator. By prioritizing these factors, healthcare providers can ensure that CT Scan images meet the highest quality standards, allowing for accurate diagnosis and effective treatment [22].

Several measures have been taken to lower the radiation dose of CT scans while preserving the image quality of the observed object, one of which is by using Iterative Reconstruction (IR) algorithms. IR is an image reconstruction algorithm superior to Filtered Back Projection (FBP). FBP works on the assumption that the obtained projection data is free from noise. After mathematical processing, such as smoothing or edge sharpening, the data is projected back into the image space to form the image volume. This process is fast and can produce adequate images in most clinical conditions. However, IR permits imaging at lower doses while sustaining image quality comparable to routine dose FBP [23]. Meanwhile, when using FBP, when the radiation dose is reduced, the image reconstructed with FBP is very noisy [24].

Various IR algorithms are accessible, including those that work in image space data such as Iterative Reconstruction in Image Space (IRIS) and Adaptive Statistical Iterative Reconstruction (ASIR), as well as those that operate in raw data, such as Sinogram Affirmed Iterative Reconstruction (SAFIRE), Adaptive Iterative Dose Reduction (AIDR) 3D, and Hybrid Iterative Reconstruction (HIR). SAFIRE is an iterative reconstruction algorithm developed by Siemens, which operates based on raw data [25]. Utilization of this algorithm has been shown to reduce noise in CT images and successfully remove CT spiral artifacts. When the SAFIRE algorithm is applied in CT image reconstruction, it has the potential to significantly improve image quality, which may lead to a reduction in the radiation dose required for CT Scan. In addition, studies have shown that SAFIRE technology can reduce CT Scan dose without increasing image noise and with minimal effect on image quality [26]

SAFIRE can effectively improve image quality in various clinical imaging. So SAFIRE should be utilized to its full potential, as an innovative image reconstruction algorithm that significantly reduces image noise without losing sharpness [27] and maintain image quality and diagnostic information [28]. This is particularly important in the case of non-hemorrhagic stroke, where image noise can cause small lesions to be overlooked or misinterpreted, potentially leading

to incorrect diagnosis and inappropriate treatment. On Siemens CT scanners, SAFIRE software has five variations, namely Strength 1, Strength 2, Strength 3, Strength 4 and Strength 5. Given the context described earlier, it is important to investigate the impact of SAFIRE application on image quality and anatomical information in head CT Scan examination, especially in patients with non-hemorrhagic stroke cases.

Previous studies on abdominal CT Scan examinations have shown that preference for image reconstruction methods does not correlate with CNR values. Because CNR cannot be used as the only reference for assessing image quality [29]. Therefore, this study not only assessed CNR but also assessed SNR and anatomical information in head CT Scan Examination in non-hemorrhagic stroke so that with the addition of variables and other examinations, this study is different from previous study. This study is expected to determine whether or not there are differences in image quality and anatomical information in the use of SAFIRE Strength variations in head CT Scan in cases of non-hemorrhagic stroke so that the most optimal SAFIRE strength in producing image quality (SNR and CNR) and anatomical information can be identified. The aim of this study is to determine differences in image quality and anatomical information in head CT Scan of non-hemorrhagic stroke cases using SAFIRE Strength variations to identify the most optimal SAFIRE Strength. This study contributes to:

- Offer a more in-depth analysis of how variations in SAFIRE Strength impact image quality and anatomical details in head CT Scan examination of non-hemorrhagic stroke cases, so that it can be a reference in developing studies related to iterative reconstruction techniques in CT Scan.
- Assist radiology practitioners in determining the most optimal SAFIRE Strength to improve image quality and anatomical information in head CT Scan with non-hemorrhagic stroke cases, thereby supporting diagnostic accuracy.
- By knowing the most optimal SAFIRE Strength, this study helps enhance the efficiency and effectiveness of the diagnostic process in non-hemorrhagic stroke cases, which can ultimately improve patient clinical outcomes.

## II. MATERIALS AND METHOD

This study uses a quantitative analytical research method with an experimental approach to analyze the difference in the value of SAFIRE Strength variation on image quality and anatomical information on the results of head CT Scan examination images of non-hemorrhagic stroke cases from July - October 2024 in one of the hospitals in Surakarta. Data collection in this study has received approval from the hospital with letter number 114/RSDOI/PSDM/II/2024.

The population in this study was the raw data of all radiology patients who had performed head CT Scan with a diagnosis of non-hemorrhagic stroke during the study period. Data were collected retrospectively using the simple random sampling method, so that each patient's raw data had an equal

chance of being selected as a sample. The sample consisted of 30 patients who met the inclusion criteria, namely head CT Scan examination patients with a diagnosis of non-hemorrhagic stroke, patients age more than 18 years at the time of examination, patients were examined less than 24 hours after symptoms of non-hemorrhagic stroke, and patient medical data in the form of raw data imaging results were available and complete. Then the samples taken were head CT Scan examination patients with a diagnosis of non-hemorrhagic stroke who use the same protocol, namely supine, headfirst position, using 120 Kv, Care Dose is on, slice thickness 5 mm, using window brain, and have been reconstructed using five SAFIRE strengths namely Strength 1, Strength 2, Strength 3, Strength 4, and Strength 5. Image quality is assessed with the IndoQCT application, which is an application designed to help analyze the quality of medical images, especially CT Scan images. This application is used to calculate quantitative parameters such as SNR and CNR, which are key indicators of image quality. Meanwhile, anatomical information was evaluated through the VGA method by three radiologists with more than five years of working experience.

The statistical tests used include the normality test, then the Friedman statistical test to assess image quality and the Kruskal-Wallis statistical test to assess anatomical information. The selection of these tests were carried out based on the type of data used and the research objectives to evaluate whether or not there was a significant difference in the use of SAFIRE Strength variations. Flow diagram of the study can be seen in FIGURE 1.

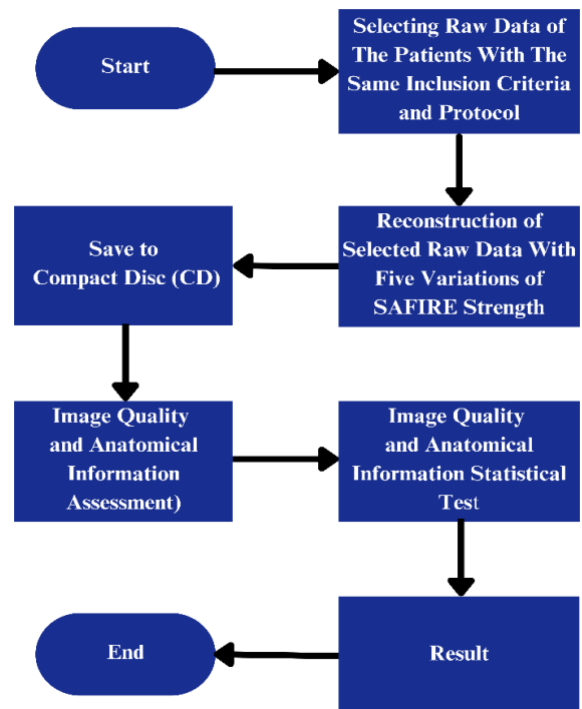


FIGURE 1. Flow diagram of the study  
 A. IMAGE RECONSTRUCTION

Image reconstruction begins by selecting raw data of head CT Scan images from 30 patients with a diagnosis of non-hemorrhagic stroke. Then raw data from the thirty patients that have been selected are reconstructed using five variations of the SAFIRE Strength iterative reconstruction algorithm, namely SAFIRE Strength 1, Strength 2, Strength 3, Strength 4, and Strength 5. This reconstruction process is carried out to produce five different sets of images for each patient, which allows comparison of image quality based on SAFIRE Strength variations. Once the reconstruction was complete, all the images were transferred to a Compact Disc (CD) storage media to facilitate the transfer process to a laptop. Furthermore, the images were analyzed using the IndoQCT application to assess image quality based on the Signal-to-Noise Ratio SNR and CNR values. Assessment of anatomical information was done through the Visual Grading Analysis (VGA) method by three radiologists, who gave scores based on the completeness and clarity of the anatomical structures seen in the images. This process ensured that each step of the study was conducted systematically to produce reliable data to evaluate the differences in image quality and anatomical information in each SAFIRE Strength

**B. IMAGE QUALITY ASSESSMENT (SNR AND CNR)**

The head CT Scan image results of each patient with non-hemorrhagic stroke cases were opened using the IndoQCT application for further analysis. The first step is to select the Low Contrast Detectability menu and then select the CNR option. After that, the ROI Object and ROI Background areas that will be used are determined with a size of 5 pixel (px) for each area. ROI Object is placed on the anatomy being assessed, while ROI Background is placed on the background area of the image. By pressing the calculate button, the calculation results in the form of SNR and CNR values will be displayed by the application. This process was carried out systematically for each anatomy in the 30 patients assessed, covering all images that had been reconstructed using the five SAFIRE Strength variations, namely Strength 1, Strength 2, Strength 3, Strength 4, and Strength 5. This approach ensures that image quality analysis is carried out in a consistent and standardized manner to obtain valid and comparable results.

Mathematically, SNR can be assessed with the following equation (Eq.(1))[30]:

$$SNR = \frac{\mu}{\sigma_{\mu}} \tag{1}$$

$\mu$  is the reconstructed attenuation coefficient for a given area, while  $\sigma_{\mu}$  is the standard deviation in the same area.

Another alternative equation for calculating SNR can be expressed using the following equation (Eq.(2))[31]:

$$SNR = \frac{HU_{average}}{\sigma_{HU}} \tag{2}$$

$HU_{average}$  is the average pixel value given in Hounsfield units in a chosen region of interest.  $\sigma_{HU}$  is the standard deviation of the pixel values within same region of interest.

Mathematically, CNR can be assessed with the following equation (Eq.(3) [32]:

$$CNR = \frac{HU_{ROI1} - HU_{ROI2}}{\sigma_{background}} \tag{3}$$

$HU_{ROI1}$  and  $HU_{ROI2}$  are average pixel values in two different chosen regions of interest.  $\sigma_{background}$  is the standard deviation of the pixel values in the background, where background may i.e. be defined as the ROI with lowest average pixel value.

**C. ANATOMICAL INFORMATION ASSESSMENT**

Analysis of differences in anatomical information from head CT Scan of non-hemorrhagic stroke patients with SAFIRE Strength variations was conducted through an assessment process by observers. In this study, three radiologists acted as observers who independently observed and assessed the CT Scan images of the patient's head directly from the computer monitor screen. The anatomical information assessed included structures such as pons, thalamus, lateral ventricle, caudate nucleus, hypodense lesion/infarct, sylvian fissure, peripheral sulci, white matter, and gray matter. The assessment process was conducted using the VGA method, with each observer placing a check mark (✓) on a questionnaire that had been prepared according to the instructions. The assessment was done using a three-level numerical system that includes scores of 1, 2, and 3, with the scores representing the clarity of the anatomical information in the image. A score of 1 indicates 'not clear', a score of 2 indicates 'less clear', and a score of 3 indicates 'clear'. These scoring were applied to all SAFIRE Strength variations for each patient to identify the reconstruction variation that provides the best anatomical information. This process was carried out systematically and consistently to ensure the accuracy and reliability of the study results. The assessment of anatomical information used the Kruskal Wallis statistical test which mathematically has the following equation (Eq.(4))[33] :

$$H = \frac{12}{NN+1} \sum n_i r_i^2 - 3N+1 \tag{4}$$

$N$  is the total number,  $n_i$  is the number in the  $i$ -th group, and  $R_i$  is the total sum of ranks in the  $i$ -th group; in the second equation  $r_i^2 = \frac{\sum r_i^2}{n_i^2}$ . Either equation can be used. The value of  $H$  is tested against the chi-square distribution for  $k - 1$  degrees of freedom, where  $k$  is the number of groups.

**TABLE 1**  
 Visual grading analysis of CT scan head in non-hemorrhagic stroke cases assessment

Score	Definition	Information
1	Not Clear	The assessed anatomy is not clear, the boundaries are not clear, and cannot be analyzed
2	Less Clear	The assessed anatomy is visible and can be analyzed but the boundaries are not clear.
3	Clear	The assessed anatomy is clearly visible, boundaries are well defined and easy to analyze.

**D. DATA ANALYSIS**

Data from the assessment of Image Quality which includes SNR and CNR parameters on CT Scan examination of the head of non-hemorrhagic stroke cases that have been assessed using the IndoQCT application were further analyzed using the Friedman statistical test, which was chosen because the data obtained were not normally distributed. In this analysis, the significance level used is p value <0.05. This means that if the p-value obtained is smaller than 0.05, the null hypothesis will be rejected, and it can be concluded that there is a significant difference in image quality produced by different SAFIRE Strength variations.

The data from the assessment of anatomical information on the head CT Scan examination for non-hemorrhagic stroke cases, which was conducted by three radiologists as observers, was also analyzed to measure the level of agreement between the observers. The three radiologists were asked to assess the anatomical information that could be extracted from the CT Scan image, which included observations on the structure and anatomical condition of the patient's head. To assess the extent to which the three observers agreed to provide an assessment, Cohen's Kappa test was used to measure the level of agreement between observers or assessors in a study. If the results of the Cohen's Kappa test statistics are less than 0.20, it is said that the suitability of opinions is poor, 0.21-0.40 is fair agreement, 0.41-0.60 is moderate agreement, 0.61-0.80 is good, and 0.81-1.00 is very good. In this study, the Kruskal-Wallis statistical test was conducted on anatomical information because the data were not normally distributed. In the context of this study, the Kruskal-Wallis test was applied to determine whether there is a significant difference in the anatomical information obtained from the use of various variations of Strength SAFIRE in the head CT Scan examination setting for non-hemorrhagic stroke cases. The level of significance applied is p value <0.05, which means that the hypothesis will be accepted if the p value obtained is smaller than 0.05, indicating a significant difference in the quality of anatomical information based on the variations of Strength SAFIRE used in the head CT Scan examination setting for non-hemorrhagic stroke cases.

**III. RESULT**

**A. IMAGE QUALITY**

**1. DIFFERENCE IN IMAGE QUALITY (SNR)**

The difference in image quality (SNR) was assessed using the Friedman statistical test because the data were not normally distributed. Friedman statistical test results can be seen in TABLE 2.

**TABLE 2**  
 Friedman statistical test results of SNR

SAFIRE	mean rank	p-value
Strength 1	1.16	0.000
Strength 2	2.16	
Strength 3	3.08	
Strength 4	3.89	
Strength 5	4.72	

The result in TABLE 2 show that the Friedman statistical test resulted in a p-value of 0.000 ( $p < 0.05$ ), indicating a significant difference between the tested groups. This finding supports the rejection of the null hypothesis ( $H_0$ ) and acceptance of the alternative hypothesis ( $H_a$ ), confirming that variations in SAFIRE Strength significantly affect image quality, as measured by CNR. Among the SAFIRE Strength variations, the highest mean rank, representing the highest CNR value, is observed at SAFIRE Strength 5, followed sequentially by Strengths 4, 3, 2, and the lowest at Strength 1. This trend is further illustrated in FIGURE 2, which visually depicts the progressive increase in CNR value with higher SAFIRE Strength levels.

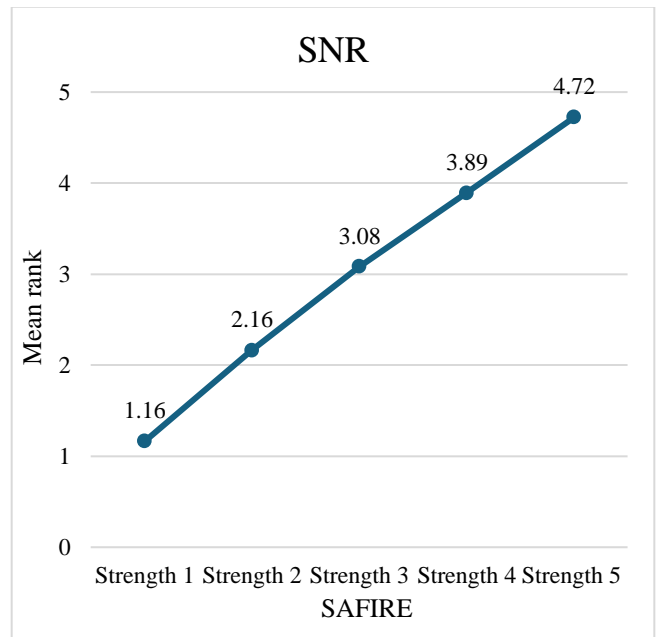


**FIGURE 2.** Mean Rank SNR Graph of Friedman statistical test results

**2. DIFFERENCE IN IMAGE QUALITY (CNR)**

The difference in image quality values (CNR) uses the Friedman statistical test because the data is not normally distributed. The Friedman test results can be seen in TABLE 3.

**TABLE 3**  
 Friedman statistical test results of CNR

SAFIRE	mean rank	p-value
Strength 1	1.56	0.000
Strength 2	1.78	
Strength 3	3.11	
Strength 4	3.78	
Strength 5	4.78	

The results in TABLE 3 indicate a p-value of 0.000 ( $p < 0.05$ ) from the Friedman statistical test, demonstrating a significant difference among the tested groups. This confirms the rejection of the null hypothesis ( $H_0$ ) and supports the alternative hypothesis ( $H_a$ ), which states that SAFIRE Strength variations significantly influence image quality as measured by CNR. The highest image quality, represented by the mean rank, is achieved with SAFIRE Strength 5, followed sequentially by Strengths 4, 3, 2, and the lowest at Strength 1. This progressive improvement in CNR with increasing SAFIRE Strength levels is also clearly depicted in FIGURE 3.

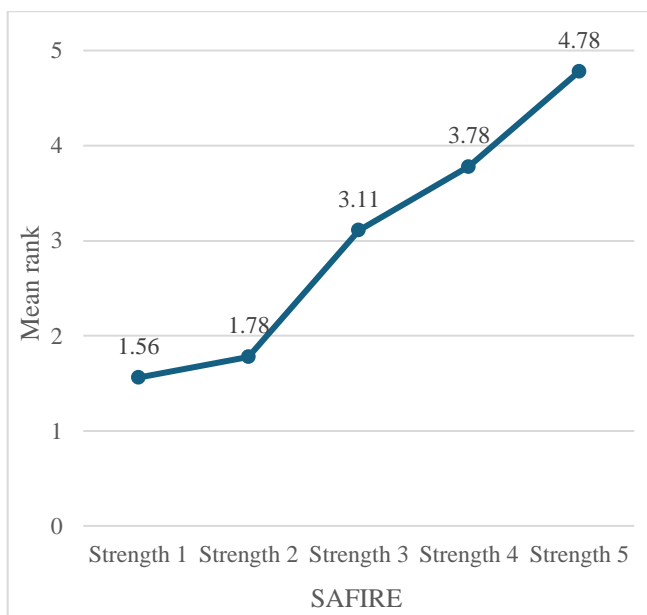


FIGURE 3. Mean rank CNR graph of Friedman statistical test results

Based on the FIGURE 4 above, it can be seen that the higher the SAFIRE Strength value will produce a smoother image because the noise is reduced. However, images that are too smooth will reduce image details. Based on the results above, it can be known that the highest mean rank for SNR and CNR values are found in the use of SAFIRE Strength 5. This shows that SAFIRE Strength 5 produces the most superior image quality compared to other SAFIRE Strength variations. The next positions are successively occupied by SAFIRE Strength 4, 3, 2, and 1. The improvement in image quality is in line with the increase in SAFIRE Strength level.

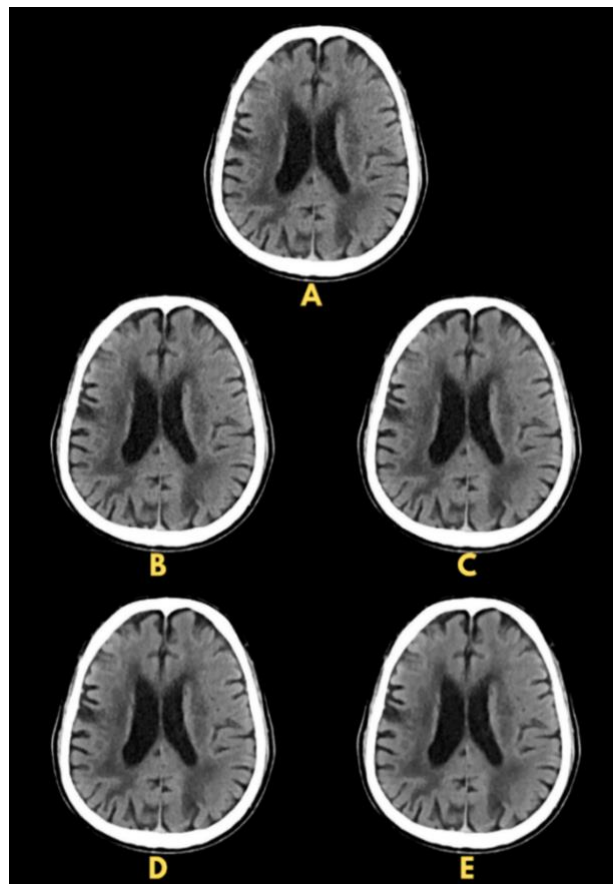


FIGURE 4. Head CT Scan Examination Images of Non-Hemorrhagic Stroke Cases With (A) Using SAFIRE Strength 1, (B) Using SAFIRE Strength 2, (C) Using SAFIRE Strength 3, (D) Using SAFIRE Strength 4, and (E) Using SAFIRE Strength 5.

**B. ANATOMICAL INFORMATION**

The assessment of anatomical information was carried out by asking three radiologists to assess the image by filling out a questionnaire for each anatomy. This research questionnaire has three scales, namely 1, 2, and 3. Value 1 states 'unclear', value 2 states 'less clear', and value 3 states 'clear'. After obtaining the scores from the radiologist, the Cohen's Kappa test was conducted using SPSS to evaluate the level of conformity or agreement between the three radiologists. The results of the Cohen's Kappa test can be seen in TABLE 4.

TABLE 4

Cohen's Kappa test results	
Observer	Value of Kappa
Observer 1 * Observer 2	0,990
Observer 1 * Observer 3	0,929
Observer 2 * Observer 3	0,939

Based on TABLE 4, it can be seen that the agreement between observers has a value of  $> 80$ , which means that the observers have a very good level of agreement. The test results show that the three observers have an objective assessment so that the researcher can use one of the assessment results from one of the observers for further testing. Therefore, the researcher used the data from the assessment of observer 2 because observer 2 has a longer

work experience as a radiologist than observer 1 and observer 3. The difference in information on each anatomy of the five SAFIRE Strength variations uses the Kruskal Wallis test because the data were not normally distributed. The results of the Kruskal-Wallis test can be seen in TABLE 5.

TABLE 5

The results of Kruskal-Wallis statistical test of information on each anatomy

Anatomy	p-value	Information
Pons	0.000	Difference
Thalamus	0.000	Difference
Ventricle Lateral	1.000	No Difference
Caudate Nucleus	0.000	Difference
Hypodense Lesion/Infarct	0.000	Difference
Sylvian Fissure	1.000	No Difference
Peripheral Sulci	1.000	No Difference
White Matter	0.000	Difference
Gray Matter	0.000	Difference

The data in TABLE 5 show that the Kruskal-Wallis test yielded a p-value of 0.000 ( $p < 0.05$ ) for several anatomical structures, including the pons, thalamus, caudate nucleus, hypodense lesion/infarct, white matter, and gray matter, indicating a significant difference in anatomical information among these structures when using different SAFIRE Strength variations. This confirms that SAFIRE Strength variations influence the quality and sharpness of anatomical details in these structures.

Conversely, for the ventricle lateral, sylvian fissure, and peripheral sulci, the Kruskal-Wallis test returned a p-value of 1.000 ( $p > 0.05$ ), suggesting no significant difference in anatomical information for these structures across the SAFIRE Strength variations. This indicates that variations in SAFIRE Strength do not affect the image quality or anatomical detail of these structures. To identify the SAFIRE Strength variation that provides the most optimal anatomical information for each structure, the mean rank values in TABLE 6 can be analyzed. These mean rank values serve as a key indicator to evaluate which SAFIRE Strength variation yields the best results for each anatomical structure. Based on TABLE 6, it can be seen that the highest mean rank is found in SAFIRE Strength 3 for the anatomy of the pons, thalamus, caudate nucleus, hypodense lesion/infarct, white matter, and gray matter which indicates that SAFIRE Strength 3 has the ability to display information on these anatomies better than other SAFIRE Strengths. Whereas in the anatomy of ventricle lateral, sylvian fissure and peripheral sulci have a constant mean rank value indicating that all SAFIRE Strengths have the same ability to display these anatomies. FIGURE 5 also presents a detailed diagram illustrating the distribution of mean rank values for each anatomical structure analyzed under the different SAFIRE Strength variations. This diagram serves as a visual representation of the comparative effectiveness of each SAFIRE Strength level in displaying anatomical details, providing a clearer understanding of the trends and disparities observed across various anatomical regions. The

visualization highlights how specific SAFIRE Strength variations perform in optimizing image quality for different anatomical structures, emphasizing their relative strengths and limitations in enhancing diagnostic accuracy.

TABLE 6

Mean rank results of Kruskal-Wallis statistical test of information on each anatomy

Anatomy	Mean Rank				
	SAFIRE Strength				
	1	2	3	4	5
Pons	61.5	61.5	131.5	61.5	61.5
Thalamus	61.5	61.5	131.5	61.5	61.5
Ventricle lateral	75.5	75.5	75.5	75.5	75.5
Caudate nucleus	61.5	61.5	131.5	61.5	61.5
Hypodense lesion/infarct	61.5	61.5	131.5	61.5	61.5
Sylvian fissure	75.5	75.5	75.5	75.5	75.5
Peripheral sulci	75.5	75.5	75.5	75.5	75.5
White matter	61.5	61.5	131.5	61.5	61.5
Gray matter	61.5	61.5	131.5	61.5	61.5

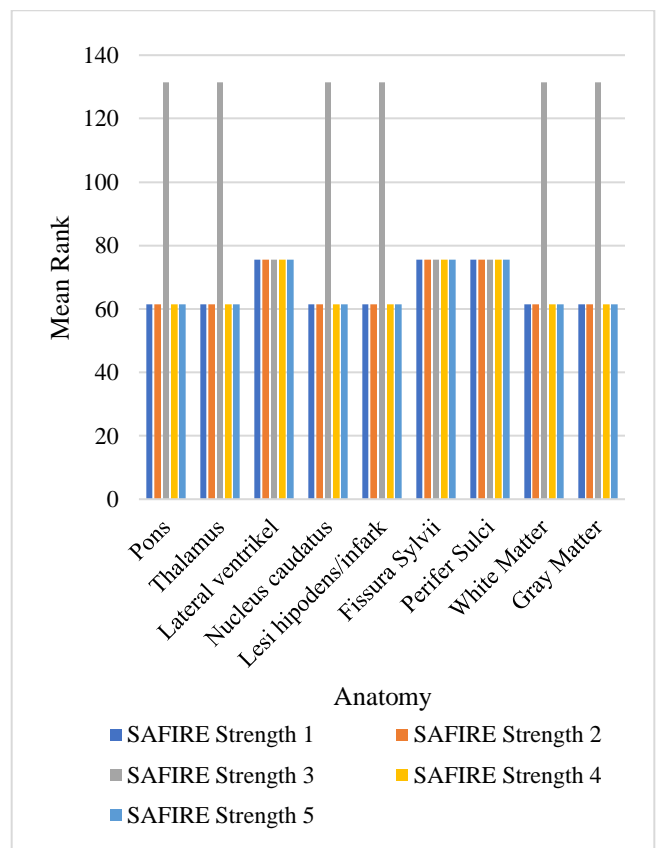
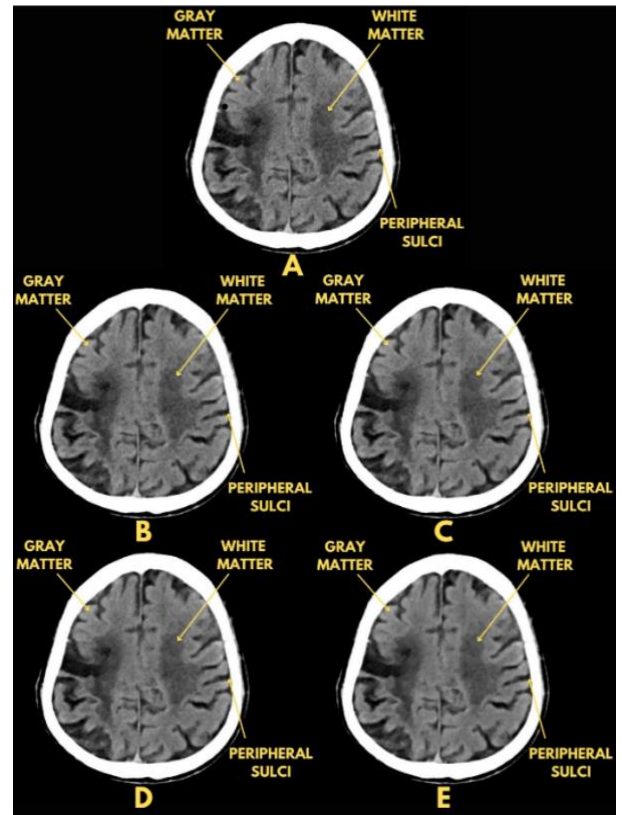


FIGURE 5. Mean rank results of Kruskal-Wallis statistical test of each anatomy



**FIGURE 6.** Anatomical Information of Pons and Hypodense Lesion/Infarct Using (A) SAFIRE Strength 1, (B) SAFIRE Strength 2, (C) SAFIRE Strength 3, (D) SAFIRE Strength 4 and (E) SAFIRE Strength 5.



**FIGURE 8.** Anatomical Information of Gray Matter, White Matter, and Peripheral Sulci With (A) Using SAFIRE Strength 1, (B) Using SAFIRE Strength 2, (C) Using SAFIRE Strength 3, (D) Using SAFIRE Strength 4 And (E) Using SAFIRE Strength 5.

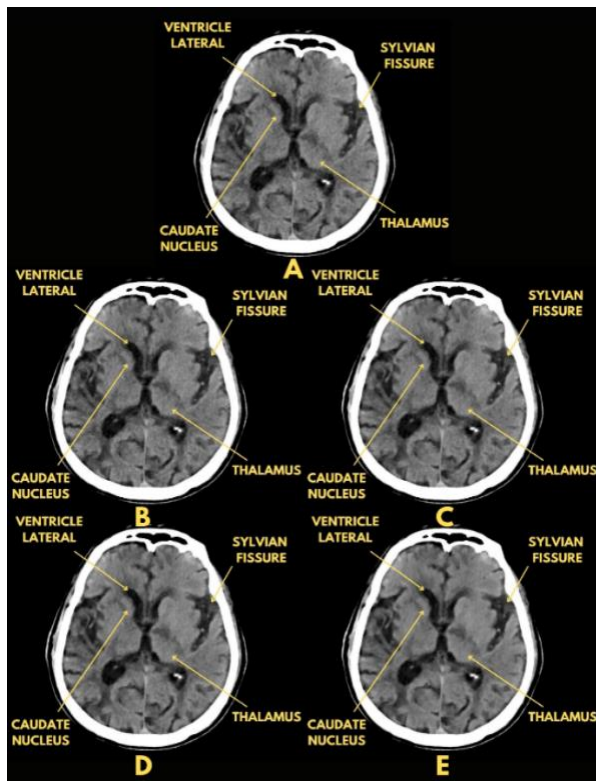


**FIGURE 7.** Anatomical Information of The Caudate Nucleus, Ventricle Lateral, Thalamus, and Sylvian Fissure Using (A) SAFIRE Strength 1, (B) SAFIRE Strength 2, (C) SAFIRE Strength 3, (D) SAFIRE Strength 4 and (E) SAFIRE Strength 5.

The difference in overall anatomical information used the Kruskal-Wallis test because the data were not normally distributed. The results of the Kruskal-Wallis test can be seen in [TABLE 7](#).

**TABLE 7**

Kruskal-Wallis statistical test results of overall anatomical information		
SAFIRE	mean rank	p-value
Strength 1	586.00	0.000
Strength 2	586.00	
Strength 3	1033.50	
Strength 4	586.00	
Strength 5	586.00	

Based on [TABLE 7](#), it can be seen that the results of the Kruskal-Wallis test obtained a p value of 0.000 ( $p < 0.05$ ), so these results indicate that  $H_0$  is rejected and  $H_a$  is accepted so that there are differences in overall anatomical information in the use of SAFIRE Strength variations. The SAFIRE Strength variation that produces the most optimal anatomical information can be seen from the mean rank value where in [FIGURE 8](#), it can be seen that the highest mean rank is in SAFIRE Strength 3 which indicates that SAFIRE Strength 3 has the ability to display the most optimal overall anatomical information compared to other SAFIRE Strengths.

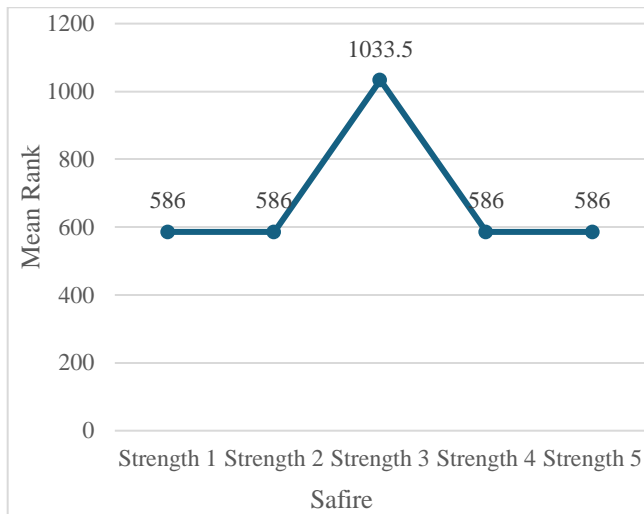


FIGURE 8. Mean rank Kruskal-Wallis statistical test results of overall anatomical information

IV. DISCUSSIONS

A. IMAGE QUALITY

This study shows that the Friedman statistical test resulted in a p-value of 0.000, which means that there is a significant difference in the SNR value in the use of SAFIRE Strength variations. From the results of the mean rank analysis, there is an increasing trend in SNR as SAFIRE Strength increases. SAFIRE Strength 1 has the lowest mean rank of 1.16 which indicates that this variation produces the lowest SNR. At SAFIRE Strength 2, the mean rank increases to 2.16 which indicates that this variation provides better SNR compared to SAFIRE Strength 1. Furthermore, at SAFIRE Strength 3 there is an increase in mean rank to 3.08 which indicates that SAFIRE Strength 3 has a higher SNR compared to the two previous variations (SAFIRE Strength 1 and SAFIRE Strength 2). The increase in mean rank continues for SAFIRE Strength 4 with a mean rank of 3.89 which indicates that this variation also provides a higher SNR improvement compared to all previous variations. SAFIRE Strength 5 has the highest mean rank of 4.72.

This study also shows that the Friedman statistical test resulted in a p-value of 0.000, which means that there is a significant difference in the CNR value in the use of SAFIRE Strength variations. From the results of the mean rank analysis, there is also a trend of improving image quality as SAFIRE Strength increases. SAFIRE Strength 1 has the lowest mean rank of 1.56 which indicates that this variation produces the lowest CNR. At SAFIRE Strength 2, the mean rank increases to 1.78 which indicates that this variation provides better image quality compared to SAFIRE Strength 1. Furthermore, at SAFIRE Strength 3 there is an increase in mean rank to 3.11 which indicates that SAFIRE Strength 3 has a higher CNR compared to the two previous variations (SAFIRE Strength 1 and SAFIRE Strength 2). The increase in mean rank continues in SAFIRE Strength 4 with a mean rank of 3.78 which indicates that this variation also provides an increase in CNR compared to all previous variations. SAFIRE Strength 5 has the highest mean rank of 4.78 which

indicates that this variation has the highest CNR value among all SAFIRE Strength variations.

This is in accordance with previous research which states that SNR and CNR value increases with each increase in SAFIRE strength variation [34][35]. The higher the signal or the lower the noise, the higher the SNR value. [23]. So that SNR has an influence on image quality where the higher the SNR value, the better the quality of the resulting image [36], [37]. Then the higher the signal or the lower the noise, the higher the CNR value [38]. Images with high CNR values are easier to use for diagnosis than images with low CNR values [39]. Therefore, the higher the CNR value, the better the image quality. This study shows that SAFIRE Strength 5 has SNR and CNR with the highest mean rank value which indicates that this variation has the best image quality among all SAFIRE Strength variations.

The image quality test results show that each SAFIRE Strength has a different ability to reduce noise. The difference in the amount of noise between SAFIRE Strength variations occurs because it is related to the SAFIRE working mechanism in reducing noise in CT Scan images. SAFIRE uses two loops, one of which occurs in sinogram space (raw data) and the other in image space. The first loop uses dynamic noise modeling technology to correct the initial deviation by reconstructing using FBP. The second loop occurs in image space, where noise is estimated and subtracted from the dataset, making the obtained image smoother. Each SAFIRE strength level has different parameters for noise regularization. Where the level of noise reduction and noise texture will change depending on the user-selected strength for each reconstruction, with strength 1 being noisier and strength 5 being smoother [27].

B. ANATOMICAL INFORMATION

In the anatomy of the pons, thalamus, caudate nucleus, hypodense lesion/infarct, white matter and gray matter, the Kruskal-Wallis test results showed a p-value of 0.000 ( $p < 0.05$ ), which statistically indicates that there is a significant difference in the quality of anatomical information generated by the use of SAFIRE Strength variations in each of these anatomies. In other words, these results indicate that variations in SAFIRE strength levels have a different effect on the ability to display anatomical information on the tested brain structures. From the mean rank analysis, it can be seen that the SAFIRE Strength 3 variation recorded the highest mean rank, which indicates that SAFIRE Strength 3 has the best ability to display and clarify anatomical information on the pons, thalamus, nucleus caudatus, hypodense/infarct lesions, white matter, and gray matter. Achieving the highest mean rank indicates that SAFIRE Strength 3 is able to produce images with more optimal quality, enabling sharper and more accurate visualization of these structures, which in turn can improve clinical interpretation and the quality of radiology analysis. In contrast, for the anatomy of the ventricles lateral, sylvian fissure, and peripheral sulci, the Kruskal-Wallis test results showed a p-value of 1.000 ( $p > 0.05$ ), indicating that there was no significant difference in the anatomical information displayed by the use of SAFIRE Strength

variations on these structures. This means that although various SAFIRE Strength variations were applied, the image quality produced for the anatomy of the ventricle lateral, sylvian fissure, and peripheral sulci showed no significant difference, and all SAFIRE Strength variations had almost similar capabilities in displaying these structures. From the mean rank analysis performed, it can be seen that the mean rank values for these three anatomies are constant across all SAFIRE Strength variations tested. This indicates that all SAFIRE Strength variations, ranging from SAFIRE Strength 1 to SAFIRE Strength 5, provide almost identical results in terms of image quality and visualization capabilities anatomy of the ventricle lateral, sylvian fissure, and peripheral sulci. Therefore, it can be concluded that for these three anatomies, none of the SAFIRE Strength variations provide a significant advantage over the others, and all variations have an equal capacity to display anatomical information.

The preference for using SAFIRE Strength 3 over other levels in CT imaging, particularly for anatomical details, comes from the balance between noise reduction and image sharpness. Studies show that moderate strength levels, such as SAFIRE Strength 3, effectively reduce image noise while maintaining adequate anatomical clarity, thus making them optimal for various clinical applications such as abdominal and lung thoracic imaging, whereas higher strengths (e.g., Strength 4 or 5) may over-smooth the image, which may result in the loss of fine and small anatomical details, thus affecting diagnostic confidence. On the other hand, lower strengths may not sufficiently suppress noise, resulting in coarser images [29].

This is in accordance with this study which can be seen that in the anatomy of the pons, thalamus, nucleus caudatus, hypodense / infarct lesions, white matter and gray matter the highest mean rank value is found in SAFIRE Strength 3, which indicates that SAFIRE Strength 3 has the most optimal ability to display this anatomical information compared to other SAFIRE Strengths. On the other hand, in the test of each anatomy above, it can be seen that there is no difference in anatomical information on the ventricle lateral, sylvian fissure and peripheral sulci. This is because these three anatomies are composed of fluid and CT scan images are not superior in distinguishing fluid collections compared to conventional imaging images [40], so the variation of SAFIRE strength in CT scan does not affect the information of these anatomies.

#### 1. Differences in Overall Anatomical Information

Based on the results of the Kruskal-Wallis test, it can be seen that there are differences in overall anatomical information on the use of SAFIRE Strength variations with a p value of 0.000 ( $<0.05$ ). From the results of the mean rank analysis, it can be seen that SAFIRE Strength with the highest mean rank is SAFIRE Strength 3 with a mean rank of 1033.50. Meanwhile, SAFIRE Strength 1, SAFIRE Strength 2, SAFIRE Strength 4, and SAFIRE Strength 5 both have a mean rank value of 586.00. This indicates that SAFIRE Strength 3 has the ability to display the most optimal overall anatomical information than other SAFIRE

Strengths.

According to research by Hardie et al., medium strength reconstruction settings (SAFIRE Strength 2 and SAFIRE Strength 3) are preferred over lower and higher strengths (SAFIRE Strength 1, SAFIRE Strength 4, and SAFIRE Strength 5) [30]. This is in accordance with the results of this study which show that there is a contradiction where SAFIRE Strength 5 has the highest SNR and CNR values among other SAFIRE Strengths, which indicates that SAFIRE Strength 5 has the best image quality among other SAFIRE Strengths. However, according to respondents, SAFIRE Strength 3 is the most optimal SAFIRE Strength in overall anatomical information, because the results of anatomical information from SAFIRE strength variations 4 and 5 look too smooth so the image details are reduced. Other studies have also shown similar things where good image quality does not necessarily display good anatomy as well, in previous studies, the use of a slice thickness of 7 mm produced good image quality but could not show firm tip boundaries and anatomical information such as the Rosen muller fossa organ, torus tuberosus, and eustachian tube could not be seen clearly due to decreased detail [41]. In this study, the case taken is non-hemorrhagic stroke, where in the case of non-hemorrhagic stroke, the image detail required must be high enough to show the infarct condition more clearly because small lesions can be missed or misinterpreted due to image noise, leading to incorrect diagnosis and potentially harmful treatment [42]. Identification of non-hemorrhagic stroke patients at high risk of developing life-threatening malignant infarction at an early stage is essential considering closer monitoring and further therapeutic measures [43]. In this study, it can be seen that SAFIRE Strength 3 infarction conditions are most clearly visible compared to other SAFIRE strength variations.

The results of this study have significant clinical implications, particularly in improving patient outcomes and diagnostic accuracy. In cases of non-hemorrhagic stroke, where identification of small infarcts is critical, SAFIRE Strength 3 offers the best balance between noise reduction and image clarity. This study supports the development of standardized CT protocols that can maximize diagnostic utility while minimizing unnecessary complexity.

This study has several limitations. First, the sample size which although statistically valid, may not be sufficient to represent all patient demographics or medical conditions. Second, the findings may also lack generalizability, as they are based on a single type of CT scanner and reconstruction algorithm, which might behave differently across various models or manufacturers. Third, this study was conducted at a single center, which could limit the applicability of its conclusions to other clinical settings with varying patient populations and imaging technologies. The last, ideally this kind of study should compare standard and low-dose examinations in the same patient. However, ethical considerations make this approach difficult to implement in real practice.

A notable observation in this study is the contradiction

between SNR/CNR values and anatomical information. While SAFIRE Strength 5 achieves the highest SNR and CNR values, it is not preferred for anatomical visualization due to excessive smoothing, which reduces the visibility of fine details. This phenomenon underscores the need to consider not only quantitative measures like SNR and CNR but also qualitative factors such as image sharpness and anatomical clarity when evaluating Iterative reconstruction techniques.

Future studies should explore the performance of SAFIRE across different anatomical regions and medical conditions to validate its utility beyond the scope of this study. Future studies may also focus on evaluating the use of other iterative reconstruction techniques in addition to SAFIRE, to determine the most efficient method in various clinical conditions.

In summary, this study demonstrates that SAFIRE Strength 3 provides the optimal balance between image quality and anatomical information, making it the preferred choice for clinical imaging in cases requiring high precision, such as non-hemorrhagic stroke. The results contribute to a better understanding of iterative reconstruction techniques, offering valuable insights for optimizing CT scan imaging protocols and improving diagnostic practices. The results of this study also provide guidance for radiology practitioners to select the optimal SAFIRE Strength level in head CT Scan examination in non-hemorrhagic stroke cases.

## V. CONCLUSION

The aim of this study is to determine differences in image quality and anatomical information in head CT scan of non-hemorrhagic stroke cases using SAFIRE variations to identify the most optimal SAFIRE Strength. This study confirms that SAFIRE Strength variations significantly affect image quality and anatomical information in head CT scan of non-hemorrhagic stroke cases. SAFIRE Strength 3 provides the optimal balance of anatomical detail, supported by a Friedman test p-value of 0.000 ( $p < 0.05$ ) for image quality and a Kruskal-Wallis test p-value of 0.000 ( $p < 0.05$ ) for anatomical structures like the pons, thalamus, and caudate nucleus, hypodense lesion/infarct, white matter, and gray matter. However, no significant differences ( $p = 1.000$ ) were found for structures like the ventricle lateral, sylvian fissure, and peripheral sulci. Although SAFIRE Strength 5 achieves the highest CNR, Strength 3 offers superior anatomical detail, making it ideal for clinical diagnostic in non-hemorrhagic stroke cases. These findings support SAFIRE Strength 3's use in practice while highlighting the need for further research into broader clinical applications.

## ACKNOWLEDGMENT

The author would like to thank all parties who have helped support and completed this research.

## REFERENCES

[1] Z. T. Al-Sharify, T. A. Al-Sharify, N. T. Al-Sharify, and H. Y. Naser, "A critical review on medical imaging techniques (CT and PET scans) in the medical field," *IOP Conf. Ser. Mater. Sci. Eng.*, vol. 870, no. 1, 2020, doi: 10.1088/1757-899X/870/1/012043.

[2] S. P. Power, F. Moloney, M. Twomey, K. James, O. J. O'Connor, and M. M. Maher, "Computed tomography and patient risk: Facts, perceptions and uncertainties," *World J. Radiol.*, vol. 8, no. 12, p. 902, 2016, doi: 10.4329/wjr.v8.i12.902.

[3] Bontrager, *Text Book of Radiographic Positioning and Related Anatomy*, Eight Edit. St. Louis, United States: Mosby Inc, 2014.

[4] M. G. George *et al.*, "CDC Grand Rounds: Public Health Strategies to Prevent and Treat Strokes.," *MMWR. Morb. Mortal. Wkly. Rep.*, vol. 66, no. 18, pp. 479–481, May 2017, doi: 10.15585/mmwr.mm6618a5.

[5] M. L. Katan Andreas, "Global Burden of Stroke," *Semin Neurol*, vol. 38, no. 02, pp. 208–211, 2018, doi: 10.1055/s-0038-1649503.

[6] F. Chen *et al.*, "Global, regional, and national burden and attributable risk factors of transport injuries: Global Burden of Disease Study 1990-2019," *Chin. Med. J. (Engl.)*, vol. 136, no. 14, pp. 1762–1764, 2023, doi: 10.1097/CM9.0000000000002744.

[7] R. Luengo-Fernandez, M. Violato, P. Candio, and J. Leal, "Economic burden of stroke across Europe: A population-based cost analysis," *Eur. Stroke J.*, vol. 5, no. 1, pp. 17–25, 2020, doi: 10.1177/2396987319883160.

[8] T. N. Rochmah, I. T. Rahmawati, M. Dahlui, W. Budiarto, and N. Bilqis, "Economic burden of stroke disease: A systematic review," *Int. J. Environ. Res. Public Health*, vol. 18, no. 14, 2021, doi: 10.3390/ijerph18147552.

[9] J. P. Smeltzer *et al.*, "Pattern of CD14+ follicular dendritic cells and PD1+ T cells independently predicts time to transformation in follicular lymphoma.," *Clin. Cancer Res.*, vol. 20, no. 11, pp. 2862–2872, 2014, doi: 10.1158/1078-0432.CCR-13-2367.

[10] C. Chugh, "Acute ischemic stroke: Management approach," *Indian J. Crit. Care Med.*, vol. 23, pp. S140–S146, 2019, doi: 10.5005/jp-journals-10071-23192.

[11] S. Yaghi *et al.*, "Lacunar stroke: Mechanisms and therapeutic implications," *J. Neurol. Neurosurg. Psychiatry*, vol. 92, no. 8, pp. 823–830, 2021, doi: 10.1136/jnnp-2021-326308.

[12] S. K. Feske, "Ischemic Stroke.," *Am. J. Med.*, vol. 134, no. 12, pp. 1457–1464, Dec. 2021, doi: 10.1016/j.amjmed.2021.07.027.

[13] V. L. Feigin *et al.*, "World Stroke Organization (WSO): Global Stroke Fact Sheet 2022," *Int. J. Stroke*, vol. 17, no. 1, pp. 18–29, Jan. 2022, doi: 10.1177/17474930211065917.

[14] S. J. Mendelson and S. Prabhakaran, "Diagnosis and Management of Transient Ischemic Attack and Acute Ischemic Stroke: A Review," *JAMA*, vol. 325, no. 11, pp. 1088–1098, Mar. 2021, doi: 10.1001/jama.2020.26867.

[15] S. Tabrizi, E. Zafar, and H. Rafiei, "A cohort retrospective study on computed tomography scan among pediatric minor head trauma patients," *Int. J. Surg. Open*, vol. 29, pp. 50–54, 2021, doi: 10.1016/j.ijso.2021.01.005.

[16] M. M. Abuzaid, W. Elshami, A. Sulieman, and D. Bradley, "Cumulative radiation exposure, effective and organ dose estimation from multiple head CT scans in stroke patients," *Radiat. Phys. Chem.*, vol. 199, p. 110306, 2022, doi: https://doi.org/10.1016/j.radphyschem.2022.110306.

[17] E. Seeram, *Computed Tomography Physical Principles, Clinical Applications, and Quality Control*, Fourth Edi. Philadelphia: W.B. Saunders Company, 2016.

[18] D. Khoramian, S. Sistani, and R. A. Firouzjah, "Assessment and comparison of radiation dose and image quality in multi-detector CT scanners in non-contrast head and neck examinations," *Polish J. Radiol.*, vol. 84, pp. e61–e67, 2019, doi: 10.5114/pjr.2019.82743.

[19] J. B. Solomon, X. Li, and E. Samei, "Relating Noise to image quality indicators in CT examinations with tube current modulation," *Am. J. Roentgenol.*, vol. 200, no. 3, pp. 592–600, 2013, doi: 10.2214/AJR.12.8580.

[20] S. Shetewi, B. Mutairi, and S. Bafaraj, "The Role of Imaging in Examining Neurological Disorders; Assessing Brain, Stroke, and Neurological Disorders Using CT and MRI Imaging," *Adv. Comput. Tomogr.*, vol. 09, pp. 1–11, Jan. 2020, doi: 10.4236/act.2020.91001.

[21] D. C. Ugwuanyi *et al.*, "Evaluation of common findings in brain computerized tomography (CT) scan: A single center study," *AIMS Neurosci.*, vol. 7, no. 3, pp. 311–318, 2020, doi: 10.3934/NEUROSCIENCE.2020017.

[22] The American College of Radiology, "Acr–Asnr–Spr Practice Parameter for the Performance of Computed Tomography (Ct) of the Head," vol. 1076, pp. 1–13, 2020.

[23] M. Staniszevska and D. Chrusciak, "Iterative reconstruction as a method for optimisation of computed tomography procedures," *Polish J. Radiol.*, vol. 82, pp. 792–797, 2017, doi: 10.12659/PJR.903557.

[24] M. J. Willemink *et al.*, "Iterative reconstruction techniques for computed tomography Part 1: Technical principles," *Eur. Radiol.*, vol. 23, no. 6, pp. 1623–1631, 2013, doi: 10.1007/s00330-012-2765-y.

[25] S. Choy *et al.*, "Comparison of image noise and image quality between full-dose abdominal computed tomography scans reconstructed with weighted filtered back projection and half-dose scans reconstructed with improved sinogram-affirmed iterative reconstruction (SAFIRE\*)," *Abdom. Radiol.*, vol. 44, no. 1, pp. 355–361, 2019, doi: 10.1007/s00261-018-1687-9.

[26] T. Wang, Y. Gong, Y. Shi, R. Hua, and Q. Zhang, "Feasibility of dual-low scheme combined with iterative reconstruction technique in acute cerebral infarction volume CT whole brain perfusion imaging," *Exp. Ther. Med.*, vol. 14, no. 1, pp. 163–168, 2017, doi: 10.3892/etm.2017.4451.

[27] K. Grant and R. Raupach, "SAFIRE: Sinogram Affirmed Iterative Reconstruction," *Tech. Rep.*, pp. 1–8, 2013.

[28] M. Scharf *et al.*, "Image quality, diagnostic accuracy, and potential for radiation dose reduction in thoracoabdominal CT, using Sinogram Affirmed Iterative Reconstruction (SAFIRE) technique in a longitudinal study," *PLoS One*, vol. 12, no. 7, pp. 1–13, 2017, doi: 10.1371/journal.pone.0180302.

[29] A. D. Hardie, R. M. Nelson, R. Egbert, W. J. Rieter, and S. V. Tipnis, "What is the preferred strength setting of the sinogram-affirmed iterative reconstruction algorithm in abdominal CT imaging?," *Radiol. Phys. Technol.*, vol. 8, no. 1, pp. 60–63, 2015, doi: 10.1007/s12194-014-0288-8.

[30] M. (Ed.). Flower, "Webb's Physics of Medical Imaging (2nd ed.)," *CRC Press*, 2012, doi: https://doi.org/10.1201/b12218.

[31] C. von Falck *et al.*, "Influence of Sinogram Affirmed Iterative Reconstruction of CT Data on Image Noise Characteristics and Low-Contrast Detectability: An Objective Approach," *PLoS One*, vol. 8, no. 2, pp. 1–10, 2013, doi: 10.1371/journal.pone.0056875.

[32] A. Winklehner *et al.*, "Raw data-based iterative reconstruction in body CTA: Evaluation of radiation dose saving potential," *Eur. Radiol.*, vol. 21, no. 12, pp. 2521–2526, 2011, doi: 10.1007/s00330-011-2227-y.

[33] J. I. E. Hoffman, "Analysis of Variance. I. One-Way," *Basic Biostat. Med. Biomed. Pract.*, pp. 391–417, 2019, doi: 10.1016/b978-0-12-817084-7.00025-5.

[34] S. S. Halliburton, Y. Tanabe, S. Partovi, and P. Rajiah, "The role of advanced reconstruction algorithms in cardiac CT," *Cardiovasc. Diagn. Ther.*, vol. 7, no. 5, pp. 527–538, 2017, doi: 10.21037/cdt.2017.08.12.

[35] A. Ahmed *et al.*, "Review article – The impact of Sinogram-Affirmed Iterative Reconstruction on patient dose and image quality compared to filtered back projection: a narrative review," *Optimax 2014*, pp. 21–26, 2015.

[36] I. Elyasi, M. A. Pourmina, and M. S. Moin, "Speckle reduction in breast cancer ultrasound images by using homogeneity modified bayes shrink," *Meas. J. Int. Meas. Confed.*, vol. 91, pp. 55–65, 2016, doi: 10.1016/j.measurement.2016.05.025.

[37] W. A. Mustafa, H. Yazid, and S. Bin Yaacob, "Illumination correction of retinal images using superimpose low pass and Gaussian filtering," *Proc. - 2015 2nd Int. Conf. Biomed. Eng. ICoBE 2015*, no. March, pp. 30–31, 2015, doi: 10.1109/ICoBE.2015.7235889.

[38] M. Welvaert and Y. Rosseel, "On the definition of signal-to-noise ratio and contrast-to-noise ratio for fMRI data," *PLoS One*, vol. 8, no. 11, 2013, doi: 10.1371/journal.pone.0077089.

[39] J. M. Kofler *et al.*, "Assessment of Low-Contrast Resolution for the American College of Radiology Computed Tomographic Accreditation Program: What Is the Impact of Iterative Reconstruction?," *J. Comput. Assist. Tomogr.*, vol. 39, no. 4, pp. 619–623, 2015, doi: 10.1097/RCT.0000000000000245.

[40] H. J. Meyer *et al.*, "CT Texture analysis and CT scores for characterization of fluid collections," *BMC Med. Imaging*, vol. 21, no. 1, pp. 1–10, 2021, doi: 10.1186/s12880-021-00718-w.

[41] A. A. D. Rachmani, S. Masrochah, and S. Mulyati, "the Difference of Anatomical Information and Image Quality of Nasopharynx

Carcinoma Ct Scan With Slice Thickness Variation on Axial Slice in Rsud Dr Moewardi Surakarta," *J. Imejing Diagnostik*, vol. 4, no. 2, p. 56, 2018, doi: 10.31983/jimed.v4i2.3992.

[42] I. P. E. Juliantara, A. L. Martoyo, and M. S. Pratista, "Safire Strength Optimization: Effect on Tissue Contrast and Pathological Assessment of Brain Msct With Non-Hemorrhage Stroke (Snh)," *J. Vocat. Heal. Stud.*, vol. 7, no. 3, pp. 142–150, 2024, doi: 10.20473/jvhs.v7.i3.2024.142-150.

[43] M. Bechstein *et al.*, "Computed Tomography Based Score of Early Ischemic Changes Predicts Malignant Infarction," *Front. Neurol.*, vol. 12, no. June, pp. 1–10, 2021, doi: 10.3389/fneur.2021.669828.

## AUTHORS BIOGRAPHY



**Alan Samudra** was born in Purbalingga, Indonesia, on August 1, 2002. He completed his secondary education at SMA Negeri 1 Rembang, where he majored in mathematics and natural sciences. In 2021, He pursued higher education at the Department of Radiologic Imaging Technology, Faculty of Health Science, University of Muhammadiyah Purwokerto (UMP). During his studies, he focused on the principles and advancements in medical imaging technology, particularly in radiologic imaging. He is passionate about contributing to the healthcare field by utilizing innovative imaging techniques to support accurate diagnosis and improve patient outcomes. His research interests include image processing, digital imaging, Computed Tomography Scan, Magnetic Resonance Imaging and diagnostic.



**Lutfatul Fitriana** was born in Purbalingga, Indonesia on March 3, 1995. She received Bachelor of Applied Health Science Radiology from Semarang Health Polytechnic Of Ministry Of Health, Indonesia in 2016. In 2017, she obtained his Master of Applied in Diagnostic Imaging (M.Tr.ID.) from Semarang Health Polytechnic Of Ministry Of Health, Indonesia. She started working as Lecturer at Department of Radiology Imaging Technology, Faculty of Health Science, University of Muhammadiyah Purwokerto (UMP) in 2019. Her research interests include image processing, digital imaging, CT Scan and diagnostic.



**Fathur Rachman Hidayat** was born in Banyumas, Indonesia on November 21, 1999. He received Bachelor of Applied Health Science Radiology from Semarang Health Polytechnic Of Ministry Of Health, Indonesia in 2021. In 2023, he obtained his Master of Applied in Diagnostic Imaging (M.Tr.ID.) from Semarang Health Polytechnic Of Ministry Of Health, Indonesia. He started working as lecturer at Department of Radiology Imaging Technology, Faculty of Health Science, University of Muhammadiyah Purwokerto (UMP) in 2024. His research interests include image processing, digital imaging, artificial intelligence, MRI and diagnostic.



**Kusananto Mukti Wibowo** was born in Sukoharjo, Indonesia on December 18, 1991. He received Bachelor of Science degree from Sebelas Maret University, Indonesia in 2013. In 2018, he obtained his Master of Engineering (M.Eng.) from University Tun Hussein Onn Malaysia (UTHM), Johor, Malaysia. He started working as Lecturer at Department of Medical Electronic Engineering Technology, Faculty of Health Science, University of Muhammadiyah Purwokerto (UMP) in 2020. His research interests include sensor, biosensor and diagnostic.



**Ariesma Githa Giovany** was born in Sragen, Indonesia, on April 5, 2001. She earned the degree of A.Md.Kes., signifying her completion of the Diploma III Program in Radiology, from Universitas Widya Husada, Semarang, Indonesia, in 2022. Shortly after graduating, she began her professional career as a radiographer at Department of Radiology at Ibnu Sina Sragen Hospital, where she worked from 2022 to 2023.

In 2023, she transitioned to the Department of Radiology at Kandang Sapi Solo Hospital. As a skilled radiographer, she operates advanced imaging equipment, including conventional X-ray machines, Computed Tomography (CT) scan, and Magnetic Resonance Imaging (MRI), contributing significantly to accurate diagnostic processes and patient care.



**Wahyu Caesarendra, Ph.D.** he has been an Assistant Professor at the Faculty of Integrated Technologies, Universiti Brunei Darussalam since October 2018 to 2024. Currently, he works at Department of Mechanical and Mechatronics Engineering, Faculty of Engineering and Science, Curtin University Malaysia, Lot 13149, Block 5 Kuala Baram Land District, CDT 250, 98009 Miri, Sarawak, Malaysia. He received a Doctor of Philosophy degree from the University of Wollongong in 2015.

He worked as a Postdoctoral Research Fellow in Rolls-Royce@NTU Corp Lab, School of Mechanical and Aerospace Engineering, Nanyang Technological University, Singapore from February 2017 to September 2018. In 2011, Wahyu Caesarendra was awarded of University Postgraduate Award and International Postgraduate Tuition Award from the University of Wollongong. He worked in the automotive and electrical company before joining Diponegoro University as a Lecturer in 2007. He was a Visiting Assistant Professor at National Taiwan University of Science and Technology from August 5-11, 2019. He has authored more than 160 research articles in Journals and Conference proceedings. He is also an academic and a guest editor in peer-reviewed journals. His research interest includes mechanical vibration, mechatronics and robotics, machine learning, and deep learning, mechanical design and 3D printing, intelligent manufacturing, and IoT. He was also a visiting researcher at the Faculty of Mechanical Engineering, Opole University of Technology, Poland from July – August 2023. He can be contacted at email: [wahyu.caesarendra@ubd.edu.bn](mailto:wahyu.caesarendra@ubd.edu.bn).